Synthesis of Quaternary Semiconductor Nanocrystals with Tunable Band Gaps

Daocheng Pan,[†] Xiaolei Wang,[†] Z. Hong Zhou,[‡] Wei Chen,[§] Chuanlai Xu,*[,§] and Yunfeng Lu*[,†]

Department of Chemical and Biomolecular Engineering and Department of Microbiology, Immunology, & Molecular Genetics, California NanoSystems Institute University of California, Los Angeles, California 90095, and School of Food Science & Technology, Jiangnan University, Wuxi Jiangsu, 214122, P.R. China

Received February 13, 2009. Revised Manuscript Received April 1, 2009

Dispersible quaternary $Cu_{1.0}Ga_xIn_{2-x}S_{3.5}$ and $Cu_{1.0}In_xTl_{2-x}S_{3.5}$ nanocrystals were successfully prepared by a toluene-thermal and a hot-injection approach and characterized using UV−vis spectroscopy, X-ray powder diffraction (XRD), and transmission electron microscopy (TEM). UV−vis absorption spectra of $Cu_{1.0}Ga_xIn_{2-x}S_{3.5}$ nanocrystals revealed that the band gaps of alloyed nanocrystals can be precisely adjusted in the range of 1.43 to 2.42 eV by increasing the indium content. From XRD analysis, the lattice parameters of $Cu_{1.0}Ga_xIn_{2-x}S_{3.5}$ nanocrystals decreased linearly with an increase in the Ga/(Ga + In) ratio in accordance with Vegard's law, which confirmed that alloyed nanocrystals have a homogeneous structure. Alloyed $Cu_{1.0}Ga_xIn_{2-x}S_{3.5}$ and $Cu_{1.0}In_xTl_{2-x}S_{3.5}$ nanocrystals have a narrow size distribution according to TEM analysis results. Moreover, it was found that oleylamine played an important role in the formation quaternary homogeneous $Cu_{1.0}Ga_xIn_{2-x}S_{3.5}$ and $Cu_{1.0}In_xTl_{2-x}S_{3.5}$ nanocrystals due to eliminating the reactivity difference of copper, gallium, and indium as well as thallium precursors.

Introduction

Multiple component chalcopyrite semiconductors, such as $CuGa_xIn_{1-x}Se_2$ (CIGS), have been regarded as one of the most promising materials for photovoltaics because of their low toxicity and high conversion efficiency.[1−4] Current manufacture of such multiple-component-chalcopyrite-based photovoltaics, however, requires the use of high-cost vacuum deposition techniques.[1−4] To reduce the processing cost, various wet-chemical approaches, such as spin-casting,[5] dip-coating,[6] and printing,[7] have been explored, which has driven intensive research in the synthesis of high quality chalcopyrite colloidal nanocrystals.[8]

To maximize the conversion efficiency, practical solar cell devices generally require their absorber materials with an optimum band gap.[9] For example, a single-junction cell requires the optimum band gap of 1.3 eV while a two-junction solar cell may require the optimum band gaps of 1.9 and 1.0 eV for two types of absorber materials, respectively.[9] These band gap requirements therefore demand the synthesis of nanocrystals with tunable band gaps. Generally, band gaps of semiconductor nanocrystals may be controlled by the size or composition.[10−16] The size-dependent band gap of quantum dots is well-known and has been widely studied; however, such a size-dependent property will be vanished after these nanocrystals are deposited and converted into a dense film. Controlling the composition of nanocrystals therefore is essential for band gap control for solar cell application. To date, several multicomponent chalcopyrite nanocrystals with tunable band gaps have been

* Corresponding authors. Email: xcl@jiangnan.edu.cn; luucla@ucla.edu.
[†] Department of Chemical and Biomolecular Engineering, California NanoSystems Institute University of California.
[‡] Department of Microbiology, Immunology, & Molecular Genetics, California NanoSystems Institute University of California.
[§] Jiangnan University.

(1) Paulson, P. D.; Haimbodi, M. W.; Marsillac, S.; Birkmire, R. W.; Shafarmana, W. N. *J. Appl. Phys.* **2002**, *91*, 10153.
(2) Marsillac, S.; Paulson, P. D.; Haimbodi, M. W.; Birkmire, R. W.; Shafarman, W. N. *Appl. Phys. Lett.* **2002**, *81*, 1350.
(3) Ramanathan, K.; Contreras, M. A.; Perkins, C. L.; Asher, S.; Hasoon, F. S.; Keane, J.; Young, D.; Romero, M.; Metzger, W.; Noufi, R.; Ward, J.; Duda, A. *Prog. Photovoltaics: Res. Appl.* **2003**, *11*, 225.
(4) Repins, I.; Contreras, M. A.; Egaas, B.; DeHart, C.; Scharf, J.; Perkins, C. L.; To, B.; Noufi, R. *Prog. Photovoltaics: Res. Appl.* **2008**, *16*, 235.
(5) Mitzi, D. B.; Yuan, M.; Liu, W.; Kellock, A. J.; Chey, S. J.; Deline, V.; Schrott, A. G. *Adv. Mater.* **2008**, *20*, 3657.
(6) Luther, J. M.; Law, M.; Beard, M. C.; Song, Q.; Reese, M. O.; Ellingson, R. J.; Nozik, A. J. *Nano Lett.* **2008**, *8*, 3488.
(7) Panthani, M. G.; Akhavan, V.; Goodfellow, B.; Schmidtke, J. P.; Dunn, L.; Dodabalapur, A.; Barbara, P. F.; Korgel, B. A. *J. Am. Chem. Soc.* **2008**, *130*, 16770.
(8) (a) Castro, S. L.; Bailey, S. G.; Raffaelle, R. P.; Banger, K. K.; Hepp, A. F. *Chem. Mater.* **2003**, *15*, 3142. (b) Zhong, H.; Zhou, Y.; Ye, M.; He, Y.; Ye, J.; He, C.; Yang, C.; Li, Y. *Chem. Mater.* **2008**, *20*, 6434. (c) Wang, D.; Zheng, W.; Hao, C.; Peng, Q.; Li, Y. *Chem. Commun.* **2008**, 2556. (d) Du, W. M.; Qian, X. F.; Yin, J.; Gong, Q. *Chem.—Eur. J.* **2007**, *13*, 8840.
(9) Vos, A. D. *J. Phys. D: Appl. Phys.* **1980**, *13*, 839.
(10) Coe, S.; Woo, W. K.; Bawendi, M.; Bulovic, V. *Nature (London)* **2002**, *420*, 800.
(11) Coe, S.; Woo, W. K.; Steckel, J. S.; Bawendi, M.; Bulovic, V. *Org. Electron.* **2003**, *4*, 123.
(12) Zhong, X. H.; Feng, Y. Y.; Knoll, W. G.; Han, M. Y. *J. Am. Chem. Soc.* **2003**, *125*, 13559.
(13) Kuykendall, T.; Ulrich, P.; Aloni, S.; Yang, P. D. *Nat. Mater.* **2007**, *6*, 951.
(14) Shafarman, W. N.; Klenk, R.; McCandless, B. E. *J. Appl. Phys.* **1996**, *79*, 7324.
(15) Tang, J.; Hinds, S.; Kelley, S. O.; Sargent, E. H. *Chem. Mater.* **2008**, *20*, 6906.
(16) Nakamura, H.; Kato, W.; Uehara, M.; Nose, K.; Omata, T.; Otsuka-Yao-Matsuo, S.; Miyazaki, M.; Maeda, H. *Chem. Mater.* **2006**, *18*, 3330.

10.1021/cm900439m CCC: $40.75
Published on Web 05/04/2009

synthesized;[7,15] however, the synthesis of such multiple component nanocrystals has been limited by reactivity difference of the precursors and the ease of phase separation of the alloy constituents.[7,15] Similar reactivities of the precursors and the small lattice mismatch are generally required to synthesize multiple component alloyed nanocrystals.

We recently reported the synthesis of high quality Cu−In−S nanocrystals with a cubic and hexagonal structure and tunable copper to indium ratio.[17] Copper diethyldithiocarbamate ($Cu(dedc)_2$) and $In(dedc)_3$ were used as precursors, and oleylamine was used as an activation agent that can expedite the precursor decomposition process. The use of oleylamine helps to eliminate the reactivity difference of the precursors and benefits the formation of the homogeneous ternary $Cu_xIn_yS_{0.5x+1.5y}$ nanocrystals. The band gaps of the $Cu_xIn_yS_{0.5x+1.5y}$ nanocrystals, however, were almost the same when the ratios of Cu to In were changed from 1:3 to 3:1.[17] In this work, band gap sensitive elements, gallium and thallium, were introduced into the $Cu_{1.0}In_{2.0}S_{3.5}$ nanocrystals to form homogeneous quaternary $Cu_{1.0}Ga_xIn_{2-x}S_{3.5}$ and $Cu_{1.0}In_xTl_{2-x}S_{3.5}$ ($0 \le x \le 2$) nanocrystals. The influence of the gallium and thallium on their band gaps and lattice parameters was also discussed. It was found that the introduction of gallium and thallium enables precise tuning of the band gaps from 1.37 to 2.42 eV. Such tunable-band-gap materials may allow precise control over the emission and absorption wavelengths, which is of interest for applications for photovoltaics,[1−4] light-emitting diodes (LEDs),[10,11] and other applications.

Experimental Section

I. Chemicals. $CuCl_2$, $GaCl_3$, $InCl_3$, $TlCl_3$, oleic acid (90%), oleylamine (70%), toluene (99.5%), octadecene (ODE, 90%), and sodium diethyldithiocarbamate (dedc) (NaS_2CNEt_2) (98%) were purchased from Aldrich.

II. Synthesis of $Cu(dedc)_2$, $Ga(dedc)_3$, $In(dedc)_3$, and $Tl(dedc)_3$. In a typical synthesis of $Cu(dedc)_2$, 2.25 g (10 mmol) of sodium diethyldithiocarbamate (Na-dedc) (NaS_2CNEt_2) was dissolved in 100 mL of water. A solution with 5 mmol of $CuCl_2$ in 50 mL of water was dropped under magnetic stirring conditions. The brown precipitate was washed with water three times and dried in an oven to remove water. $Ga(dedc)_3$, $In(dedc)_3$, and $Tl(dedc)_3$ were made using the same procedure.

III. Synthesis of $Cu_{1.0}Ga_xIn_{2-x}S_{3.5}$ ($0 \le x \le 2$) Nanocrystals by a Toluene-Thermal Approach. For the synthesis of $Cu_{1.0}Ga_{1.0}In_{1.0}S_{3.5}$ nanocrystals, 9.0 mg (0.025 mmol) of $Cu(dedc)_2$, 13.3 mg (0.025 mmol) of $Ga(dedc)_3$, 14.0 mg (0.025 mmol) of $In(dedc)_3$, 1.0 mL of oleic acid, and 1.0 mL of oleylamine were dissolved in 10 mL of toluene using ultrasound. The solution was placed in a Teflon lined stainless steel autoclave and reacted at 180 °C for 90 min. As formed $Cu_{1.0}Ga_{1.0}In_{1.0}S_{3.5}$ nanocrystals were precipitated from the solution by adding 30 mL of ethanol and isolated by centrifugation and decantation. The purified nanocrystals were redispersed in toluene for UV−vis, transmission electron microscopy (TEM), and X-ray diffraction (XRD) measurements.

IV. Synthesis of $Cu_{1.0}In_xTl_{2-x}S_{3.5}$ ($0 \le x \le 2$) Nanocrystals by a Hot-Injection Approach. For the synthesis of $Cu_{1.0}In_{1.0}Tl_{1.0}S_{3.5}$ nanocrystals, 9.0 mg (0.025mmol) of $Cu(dedc)_2$, 14.0 mg (0.025 mmol) of $In(dedc)_3$, 15.4 mg (0.025 mmol) of $Tl(dedc)_3$, 1.0 mL of oleic acid, and 10 mL of octadecene (ODE) were added to a 50 mL three-neck flask. This mixture was heated to 200 °C under nitrogen flow, and 1.0 mL of oleylamine was swiftly injected into the flask under magnetic stirring condition. The reaction mixture was kept at 200 °C for 1.0 min. The flask was cooled immediately to room temperature using a water bath. Insoluble solid was separated by centrifugation and decantation prior to further purification. Thirty milliliters of ethanol was used to precipitate nanocrystals. The precipitated nanocrystals were then redispersed in toluene.

V. Characterization. UV−vis absorption spectra were recorded on a Shimadzu UV-1700 spectrometer with a resolution of 1.0 nm. The powder XRD patterns were obtained using a Panalytical X'Pert Pro X-ray diffractometer. TEM image was taken on a CM-120 (FEI company) electron microscope with an accelerating voltage of 120 kV. Energy dispersive spectroscopy (EDS) spectra were obtained by using a scanning electron microscope (JEOL JSM-6700F).

Results and Discussion

A family of alloyed Cu−Ga−In−S multiple component chalcopyrite nanocrystals can be readily synthesized using the methods described above. As a result of better solubility in nonpolar solvents, such as toluene and octadecene, $Cu_{1.0}Ga_xIn_{2-x}S_{3.5}$ nanocrystals were chosen as a model system. Systematic studies on the crystalline structure, composition and morphology, electronic state, and optical property are provided below.

I. Crystalline Structure. As known, X-ray diffraction (XRD) is the most convenient and effective tool for investigation of a crystalline structure; however, the standard XRD patterns of $Cu_{1.0}Ga_{2.0}S_{3.5}$ and $Cu_{1.0}In_{2.0}S_{3.5}$ could not be found in the literature and JCPDS card database. Nevertheless, we noticed that the XRD patterns of cubic and hexagonal $Cu_xIn_yS_{0.5x+1.5y}$ nanocrystals remain unchanged when the ratios of Cu to In were adjusted broadly from 3:1 to 1:3.[17] Given their similar compositions, $Cu_{1.0}Ga_{2.0}S_{3.5}$ and $Cu_{1.0}In_{2.0}S_{3.5}$ nanocrystals should exhibit crystalline structures similar to those of the $Cu_xIn_yS_{0.5x+1.5y}$. Figure 1 shows XRD patterns of the $Cu_{1.0}Ga_{2.0}S_{3.5}$, $Cu_{1.0}In_{2.0}S_{3.5}$ and $Cu_{1.0}Ga_xIn_{2-x}S_{3.5}$ nanocrystals, which exhibit three prominent peaks consistent with the (111), (220), and (311) planes of a cubic structure. The calculated lattice mismatch between $Cu_{1.0}Ga_{2.0}S_{3.5}$ and $Cu_{1.0}In_{2.0}S_{3.5}$ is only 4.8%, making it possible to form homogenously alloyed nanocrystals. As the indium content increases, the diffraction peaks gradually shift toward lower angles, indicating a graduate increase of the lattice parameter. According to the Vegard's law, the lattice parameter c should be a linear function of composition x, $c_x = c^{(Cu_{1.0}Ga_{2.0}S_{3.5})} + (c^{(Cu_{1.0}In_{2.0}S_{3.5})} - c^{(Cu_{1.0}Ga_{2.0}S_{3.5})})x$, where c is the c-axis lattice constant of the cubic structure and x is the molar fraction of $Cu_{1.0}In_{2.0}S_{3.5}$. The lattice parameters c measured from the XRD patterns are listed in Table 1 and are in good agreement with the Vegard's law. The lattice parameters increase linearly with the indium composition (see Figure 2, red line), confirming the formation of a homogeneous alloy structure. In addition, the $Cu_{1.0}Ga_xIn_{2-x}S_{3.5}$ nanocrystals should have homogenously alloyed structure, since a mixture of $Cu_{1.0}Ga_{2.0}S_{3.5}$ and $Cu_{1.0}In_{2.0}S_{3.5}$ should show diffraction peaks with broader widths.

(17) Pan, D.; An, L.; Sun, Z.; Hou, W.; Yang, Y.; Yang, Z.; Lu, Y. *J. Am. Chem. Soc.* **2008**, *130*, 5620.

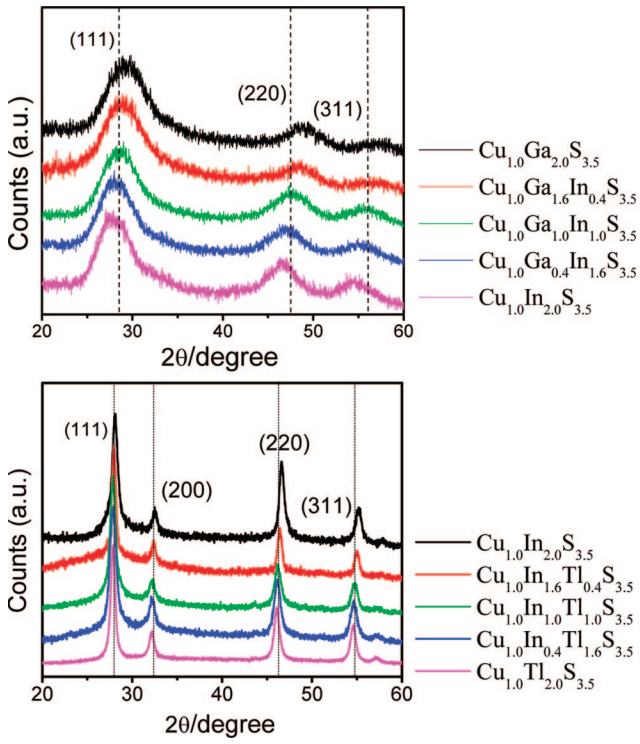

Figure 1. XRD patterns of $Cu_{1.0}Ga_xIn_{2-x}S_{3.5}$ (top) and $Cu_{1.0}In_xTl_{2-x}S_{3.5}$ (bottom) nanocrystals synthesized by a toluene-thermal approach for 90 min and a hot-injection approach for 1 min, respectively.

Table 1. Composition (from EDX Analysis), Optical Band Gaps (E_g) (from UV/Vis Spectra), and Lattice Parameter c (from XRD Patterns) of the $Cu_{1.0}Ga_xIn_{2-x}S_{3.5}$ Nanocrystals

	Cu %	Ga %	In %	S %	E_g (eV)	C (Å)
$Cu_{1.0}Ga_{2.0}S_{3.5}$	14.02	28.21		57.77	2.42	5.27342
$Cu_{1.0}Ga_{1.6}In_{0.4}S_{3.5}$	15.57	27.04	8.02	49.37	2.15	5.34015
$Cu_{1.0}Ga_{1.0}In_{1.0}S_{3.5}$	13.46	13.46	16.12	56.96	1.84	5.40237
$Cu_{1.0}Ga_{0.4}In_{1.6}S_{3.5}$	14.33	5.70	28.66	51.31	1.55	5.46609
$Cu_{1.0}In_{2.0}S_{3.5}$	14.15		27.35	58.50	1.43	5.52479

Figure 1 also shows the XRD patterns of the $Cu_{1.0}In_x$-$Tl_{2-x}S_{3.5}$ nanocrystals. Similar to the XRD patterns of the $Cu_{1.0}Ga_xIn_{2-x}S_{3.5}$ nanocrystals, the $Cu_{1.0}In_xTl_{2-x}S_{3.5}$ nanocrystals also show patterns gradually shifting toward the lower angle region with decreasing indium content, which is consistent the larger size of thallium than indium. The fwhm values (full width at half-maximum) of the five $Cu_{1.0}In_xTl_{2-x}S_{3.5}$ nanocrystal samples are similar; these nanocrystals have the similar size calculated by Scherrer

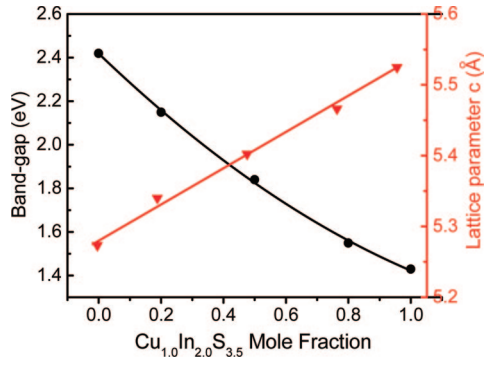

Figure 2. Lattice parameter c and optical band gap E_g of the $Cu_{1.0}Ga_xIn_{2-x}S_{3.5}$ nanocrystals as a function of $Cu_{1.0}In_{2.0}S_{3.5}$ molar fraction.

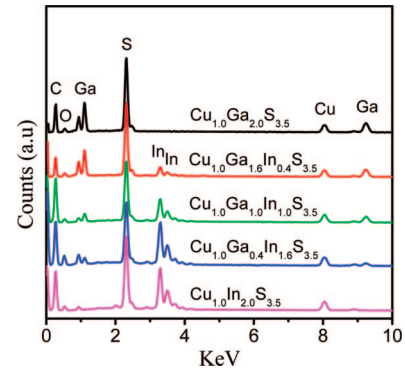

Figure 3. EDX spectra of $Cu_{1.0}Ga_{2.0}S_{3.5}$, $Cu_{1.0}In_{2.0}S_{3.5}$ and $Cu_{1.0}Ga_xIn_{2-x}S_{3.5}$ nanocrystals.

equation ($D = K\lambda/(\beta \cos \theta)$; $K = 0.89$, $\lambda = 0.154$ nm, $\beta =$ fwhm, $\theta =$ diffraction angle). The calculated particle size is about 15 nm for the $Cu_{1.0}In_{1.0}Tl_{1.0}S_{3.5}$ nanocrystals, which is very close to the size determined by TEM image.

II. Composition and Morphology. The chemical compositions of $Cu_{1.0}Ga_xIn_{2-x}S_{3.5}$ nanocrystals were analyzed by energy dispersive spectroscopy. Figure 3 shows the energy dispersive X-ray (EDX) spectra of the $Cu_{1.0}Ga_xIn_{2-x}S_{3.5}$ nanocrystals. EDX spectra indicate the presence of copper, gallium, indium, and sulfur, as well as carbon and oxygen from the oleic acid. The peak intensity of gallium gradually increases with increasing gallium content, while the intensity of indium decreases. In all cases, elemental nitrogen was not observed, indicating that oleylamine was not a capping agent. But oleylamine still played an important role in the synthesis of the nanocrystals. Oleylamine, as an organic base, can expedite the precursor decomposition process and decrease its reaction temperature. For example, no nanocrystal formation was found in the absence of oleylamine at 180 °C, and this reaction proceeded rapidly after the addition of oleylamine. Note that the thermal decomposition temperatures of the copper, gallium, and indium precursors are different according to thermogravimetric analysis (TGA) (Figure S1, Supporting Information); addition of oleylamine may also reduce their activity difference and benefit the formation of homogeneous multicomponent alloyed nanocrystals. Quantitative elemental EDX analyses of these nanocrystals are listed in Table 1. It was found that the compositions of Cu:Ga:In:S for the $Cu_{1.0}Ga_xIn_{2-x}S_{3.5}$ nanocrystals are close to those calculated from the precursors used, indicating the feasibility of controlling the nanocrystal compositions. The EDX spectra of the $Cu_{1.0}In_xTl_{2-x}S_{3.5}$ nanocrystals are given in Figure S2 (Supporting Information), and quantitative elemental analyses are also listed in Table S1 (Supporting Information).

TEM studies indicate that these nanocrystals are nearly spherical with narrow size distribution. Figure 4 (left) shows a representative TEM image of $Cu_{1.0}Ga_{1.0}In_{1.0}S_{3.5}$ nanocrystals. Nearly spherical nanoparticles with diameter around 6.2 nm and a standard size-distribution deviation of 14% can be observed. Figure 4 (right) also shows a TEM image of $Cu_{1.0}In_{1.0}Tl_{1.0}S_{3.5}$ nanocrystals synthesized by a hot-injection approach under normal pressure at 200 °C for 1.0 min. Nanocrystals having an average size of 16 nm with a relatively narrow size distribution (~7%)

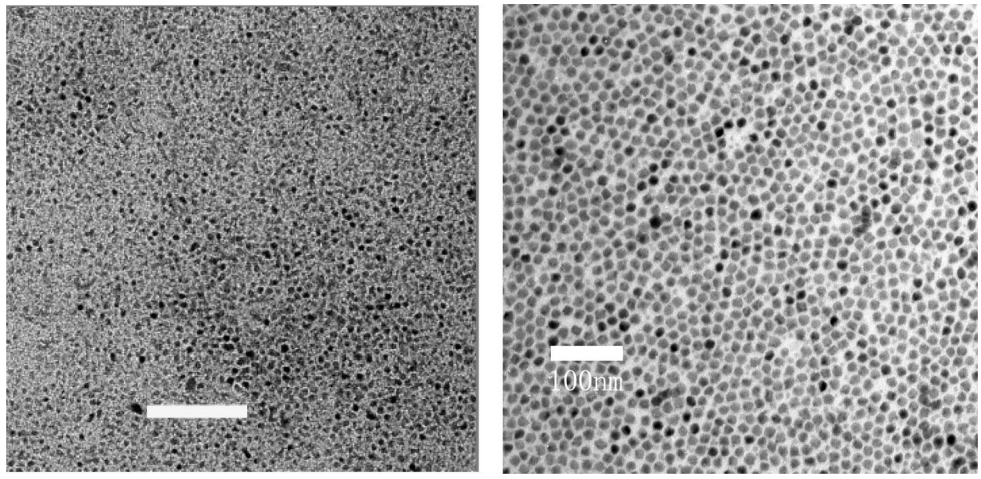

Figure 4. TEM image of (left) $Cu_{1.0}Ga_{1.0}In_{1.0}S_{3.5}$ nanocrystals synthesized by a toluene-thermal approach (scale bar is 80 nm) and (right) $Cu_{1.0}In_{1.0}Tl_{1.0}S_{3.5}$ nanocrystals synthesized by a hot-injection approach at 200 °C for 1.0 min.

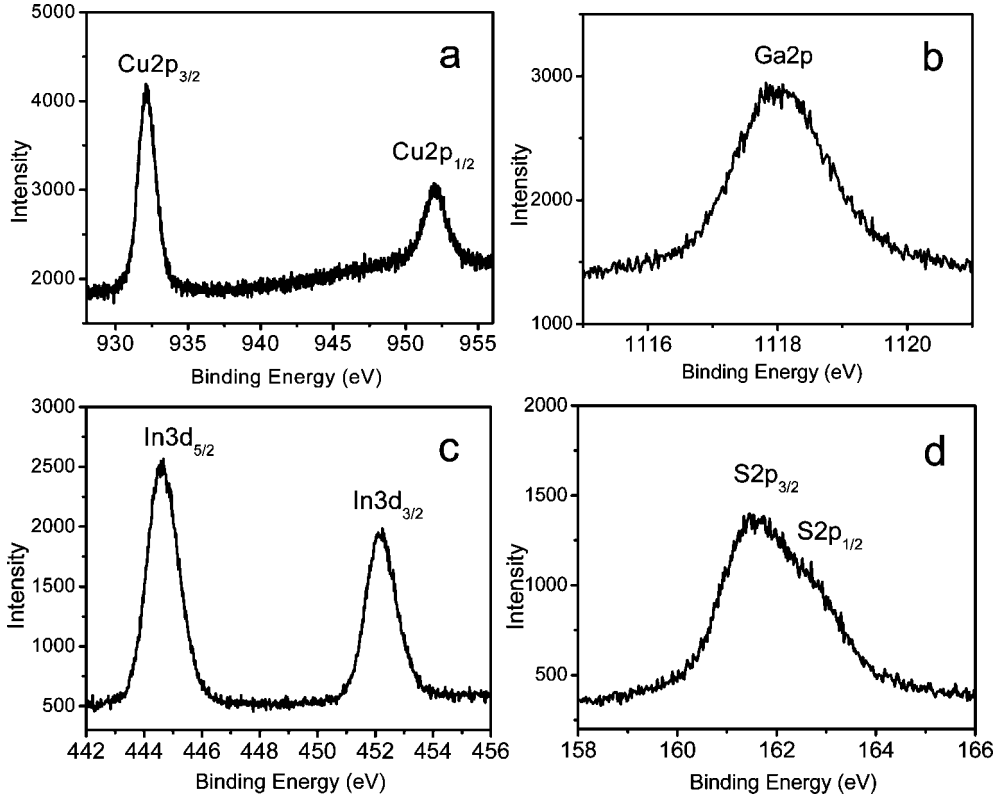

Figure 5. XPS of the oleic-acid-capped $Cu_{1.0}Ga_{1.0}In_{1.0}S_{3.5}$ nanocrystals: (a) Cu_{2p}; (b) Ga_{2p}; (c) In_{3d}; (d) S_{2p}.

are observed owing to the burst nucleation in a hot-injection reaction at high temperature. By a hot-injection approach, other $Cu_{1.0}In_xTl_{2-x}S_{3.5}$ nanocrystals with similar size and narrow size distributions could also be synthesized at the same conditions (see Figure S3, Supporting Information). Compared to the nanocrystals prepared from a toluene thermal approach, the nanocrystals prepared by a hot-injection show larger size and narrower size distribution as a result of different nucleation and growth kinetics.

III. Electronic State and Optical Measurements. The electronic states of the $Cu_{1.0}Ga_{1.0}In_{1.0}S_{3.5}$ nanocrystals were probed by the X-ray photoelectron spectroscopy (XPS). Figure 5 shows XPS spectra of the oleic acid-capped $Cu_{1.0}Ga_{1.0}In_{1.0}S_{3.5}$ nanocrystals. The Cu 2p core splits into $2p_{3/2}$ (932.1 eV) and $2p_{1/2}$ (952.0 eV) peaks. The observed binding energy of Cu 2p is in good accordance with those reported in the literature for the $CuInS_2$ nanocrystals,[17−19] suggesting that the copper valence state in the $Cu_{1.0}Ga_{1.0}In_{1.0}S_{3.5}$ nanocrystals is +1. The surface gallium ions of the nanocrystals are bonded with oleic acid, resulting in Ga−O bonds with slightly higher binding energy than that of the Ga−S bonds and broadened Ga 2p spectrum. Similarly, In 3d shows two peaks at 444.6 and 452.2 eV, consistent with a valence of +3. The two peaks located at 161.6 and 162.8 eV in Figure 5d were assigned to S 2p binding energy with a valence of −2.

(18) Muller, K.; Milko, S.; Schmeiber, D. *Thin Solid Films* **2003**, *431−432*, 312.
(19) Xiao, J. P.; Xie, Y.; Tang, R.; Qian, Y. T. *J. Solid State Chem.* **2001**, *161*, 179.

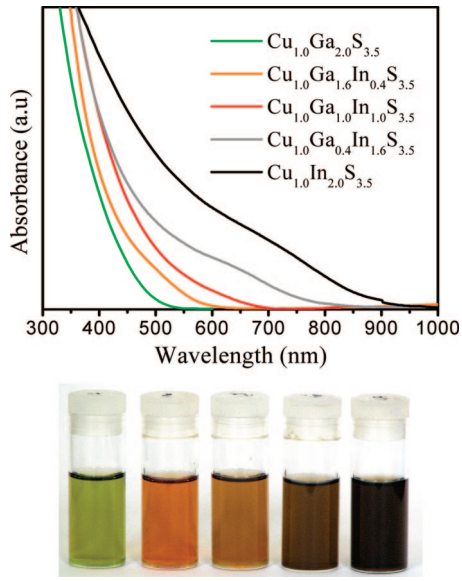

Figure 6. UV/vis absorption spectra of $Cu_{1.0}Ga_{2.0}S_{3.5}$, $Cu_{1.0}Ga_{1.6}In_{0.4}S_{3.5}$, $Cu_{1.0}Ga_{1.0}In_{1.0}S_{3.5}$, $Cu_{1.0}Ga_{0.4}In_{1.6}S_{3.5}$, and $Cu_{1.0}In_{2.0}S_{3.5}$ nanocrystals synthesized by a toluene-thermal approach and their optical micrographs showing systematically increase of optical band gaps.

Figure 6 shows UV/vis absorption spectra (top) and optical micrographs (bottom) of $Cu_{1.0}Ga_xIn_{2-x}S_{3.5}$ ($0 \le x \le 2$) nanocrystals synthesized by a toluene-thermal approach at 180 °C. With increasing the indium content, the nanocrystals dispersed in toluene change their color from green, orange, and red to black. Consistently, the band-edge absorption of the $Cu_{1.0}Ga_xIn_{2-x}S_{3.5}$ nanocrystals gradually red shifts with increasing indium composition. To further quantify the band gap evolution, Table 1 lists the optical band gaps calculated from the intercepts of the tangent of the absorption spectra. As shown in Table 1, the optical band gaps of $Cu_{1.0}Ga_{2.0}S_{3.5}$ and $Cu_{1.0}In_{2.0}S_{3.5}$ nanocrystals are around 2.42 and 1.43 eV, respectively, which are close to those of the bulk $CuGaS_2$ (2.40 eV) and $CuInS_2$ (1.50 eV). Consistent with the color change, the band gaps of the $Cu_{1.0}Ga_xIn_{2-x}S_{3.5}$ nanocrystals can be readily tuned between 2.42 and 1.43 eV by adjusting the ratios of Ga to In. The black line in Figure 2 shows the optical band gap as a function of $Cu_{1.0}In_{2.0}S_{3.5}$ molar fraction. All data points were fitted by the following modified bowing equation, where b is the bowing parameter and y is the $Cu_{1.0}In_{2.0}S_{3.5}$ molar fraction ($y = 1 - 0.5x$).

$$E_g^{(Cu_{1.0}Ga_xIn_{2-x}S_{3.5})} = E_g^{(Cu_{1.0}In_{2.0}S_{3.5})}y + E_g^{(Cu_{1.0}Ga_{2.0}S_{3.5})}(1 - y) - by(1 - y)$$

The band gap bowing parameter for $Cu_{1.0}Ga_xIn_{2-x}S_{3.5}$ ($0 \le x \le 2$) nanocrystals is around 0.42 eV, which slightly deviates from the linear relation between the band gap and the composition. This study suggests that quaternary semiconductor nanocrystals with tunable band gaps can be readily prepared using this approach. Note that $Cu_{1.0}In_xTl_{2-x}S_{3.5}$ ($0 \le x \le 2$) nanocrystals were also synthesized by a hot-injection approach; however, because of the similar band gaps of $Cu_{1.0}In_{2.0}S_{3.5}$ (1.45 eV) and $Cu_{1.0}Tl_{2.0}S_{3.5}$ (1.37 eV) nanocrystals, their alloyed nanocrystals only show slight band gap variations at different compositions (see Figure S4, Supporting Information).

Conclusion

In summary, multiple component $Cu_{1.0}Ga_xIn_{2-x}S_{3.5}$ and $Cu_{1.0}In_xTl_{2-x}S_{3.5}$ ($0 \le x \le 2$) semiconductor nanocrystals with a tunable band gap were synthesized using generic chemicals by toluene-thermal and a hot-injection approaches. Equivalent gallium or thallium were introduced into the $Cu_{1.0}In_{2.0}S_{3.5}$ nanocrystals to partly replace the indium, forming multicomponent nanocrystals with broad compositional ranges. The optical band gaps and lattice parameters of the alloyed nanocrystals are composition-dependent, following the bowing equation and Vegard's law. These nanocrystals have good solubility in common solvents and may be potentially used as absorber and window materials in multijunction photovoltaic cells and other applications.

Acknowledgment. This work was partially supported by the Chinese National Science Foundation (NSF) through CAREER, ONR, and Sandia National Laboratories. The authors would like to thank Dr. William Hou at UCLA for XPS measurement.

Supporting Information Available: TG profiles of copper, gallium, and indium precursors; EDX spectra and TEM images of $Cu_{1.0}In_xTl_{2-x}S_{3.5}$ nanocrystals (PDF). This material is available free of charge via the Internet at http://pubs.acs.org.

CM900439M